

lower $\frac{1}{3}$ of the fluid ($y \leq 10\Delta$) had $\frac{1}{3}$ the temperature and three times the density of the rest of the fluid; then in the lower area the slow-shock conditions do not apply. The forward shock front seems to be discontinued at around the $y = 10\Delta$ boundary in this case [see Fig. 3(c)]. In addition we no longer observe the quadrupole pattern but instead the pattern in Fig. 3(d).

The authors are grateful for communications with Dr. T. Taniuti, Dr. C. F. Kennel, Dr. F. Coroniti, Dr. S. Hashiguchi, Dr. K. Mima, Dr. A. Hertzberg, and Dr. H. Hasimoto. This work was supported by the National Science Foundation, Grant No. PH4-15233.

- ¹W. R. Sears, *Rev. Mod. Phys.* **32**, 701 (1960).
²H. Hasimoto, *Rev. Mod. Phys.* **32**, 860 (1960).
³A. D. Craig and J. Paul, *Phys. Rev. Lett.* **30**, 681 (1973).
⁴J. K. Chao and S. Olbert, *J. Geophys. Res.* **75**, 6394 (1970).
⁵J. N. Leboeuf, T. Tajima, and J. M. Dawson, to be published.
⁶L. Landau and E. Lifshitz, *Fluid Mechanics* (Pergamon, New York, 1959), p. 310.
⁷C. K. Birdsall, A. B. Langdon, and H. Okuda, *Methods in Computational Physics* (Academic, New York, 1970), Vol. 9, p. 241.
⁸H. Grad, *Rev. Mod. Phys.* **32**, 830 (1960).
⁹A. Jeffrey and T. Taniuti, *Nonlinear Wave Propagation* (Academic, New York, 1964), p. 293.

Observation of the Orientation Dependence of Interface Dipole Energies in Ge-GaAs

R. W. Grant, J. R. Waldrop, and E. A. Kraut

Science Center, Rockwell International, Thousand Oaks, California 91360

(Received 19 December 1977)

The interfaces between a thin ($\sim 20\text{-\AA}$) abrupt epitaxial layer of Ge grown on substrates of (111), (110), and (100) GaAs have been investigated with x-ray photoelectron spectroscopy. Observed changes in core-level binding energies have been directly related to the crystallographic orientation dependence of interface dipoles and variations of band-gap discontinuities. The orientation variation of the band-gap discontinuities is found to be a significant fraction ($\approx \frac{1}{4}$) of the total band-gap discontinuity.

There has been considerable theoretical interest in the properties of ideal abrupt interfaces between different semiconductors, stimulated in part by the recent progress in molecular beam epitaxy (MBE) whereby truly abrupt interfaces can now be achieved. A basic property of the abrupt semiconductor interface is the relative alignment of the energy bands of the two semiconductors; i.e., how the energy difference in the band gaps (ΔE_g) is distributed between the valence- and conduction-band discontinuities (ΔE_v and ΔE_c) such that $\Delta E_g = \Delta E_v + \Delta E_c$.

The first and most widely used model for estimating ΔE_c (or ΔE_v) is based on electron affinity differences.¹ Critical evaluations^{2,3} have been made of this model. Alternative models for predicting ΔE_v have appeared,^{4,5} and two self-consistent calculations of the Ge/GaAs-interface electronic structure have been completed.^{6,7} Although it has long been recognized that interface dipoles could produce energy-band discontinuities which depend on crystallographic orientation of the interface plane, such effects have generally been ignored. Transport measurements⁸ on vapor-grown Ge/GaAs heterojunctions suggested that

there could be substantial (a few tenths of an eV) changes in valence- and conduction-band discontinuities, $\delta(\Delta E_v)$ and $\delta(\Delta E_c)$, dependent on crystallographic orientation. Unfortunately, it is relatively difficult to determine these dopant-level-independent quantities from transport measurements and the scatter in these data is as large as the measured effect.

To investigate the interface dipole orientation dependence, we have developed a contactless x-ray photoemission spectroscopy (XPS) technique which allows a direct probe of interface potential variations. Herein, we report the observation of sizable and systematic variations in ΔE_v for the Ge/GaAs interface as a function of crystallographic orientation. Figure 1 is a schematic energy-band diagram of an ideal abrupt Ge/GaAs interface. The relative positions of the average bulk crystal potential within the two semiconductors determine ΔE_v and ΔE_c .^{2,4-6} An orientationally dependent change in the interface dipole magnitude may shift the relative positions of the valence and conduction bands in the two semiconductors as shown schematically by dashed lines in Fig. 1. Figure 1 also shows the position of a

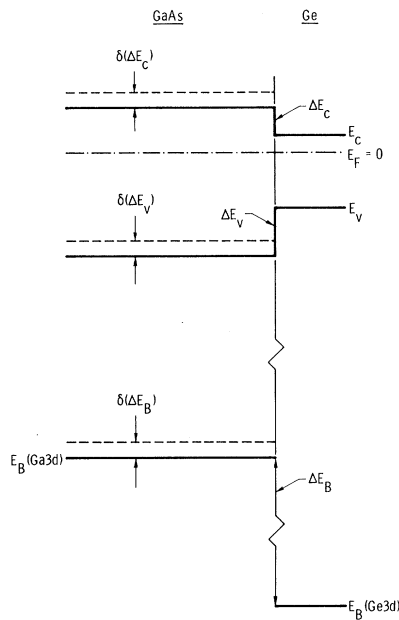


FIG. 1. Schematic energy-band diagram. The dashed lines illustrate a decreased value of ΔE_v associated with an interface dipole layer that accelerates photoelectrons from a GaAs substrate relative to Ge $3d$ photoelectrons which do not cross the interface.

core level in Ge and in GaAs. As the average bulk crystal potential changes to adjust to the dipole variation, the relative binding energies of all levels on both sides of an abrupt interface (measured relative to the common Fermi level, E_F) must also vary by the change in dipole energy with orientation; i.e., $|\delta(\Delta E_v)| = |\delta(\Delta E_c)| = |\delta(\Delta E_B)|$ also indicated by dashed lines in Fig. 1. For the Ge/GaAs interface, we will specifically consider the energy separation, ΔE_B , between the Ga $3d$ and Ge $3d$ core electron levels. A measurement of $\delta(\Delta E_B)$ by XPS thus provides a direct measure of $\delta(\Delta E_v)$. The dashed lines in Fig. 1 illustrate a change in the interface dipole which would increase the splitting between the Ga $3d$ and Ge $3d$ core levels to equal the decrease in ΔE_v .

Our experiment used Al $K\alpha$ ($h\nu = 1486.6$ eV) radiation in conjunction with an extensively modified Hewlett-Packard model 5950A ESCA (electron spectroscopy for chemical analysis) spectrometer to excite photoelectrons from Ge/GaAs interfaces for which the Ge was an ≈ 20 -Å-thick layer on a thick (≈ 0.5 mm) GaAs substrate. The escape depth for the Ge $3d$ and Ga $3d$ photoelectrons is ≈ 20 Å. Thus, photoelectrons from both sides of the Ge/GaAs interface are observed simulta-

neously in the same XPS spectrum. Electrons which originate on the GaAs side of an abrupt interface pass through any dipole layer at the interface in order to be emitted from the free surface and detected, while electrons originating in the Ge do not. For example, an electron passing through a dipole layer in a direction from higher to lower electron density will experience an acceleration and, consequently, a relative increase in kinetic energy proportional to the dipole moment per unit area, τ , at the interface.⁹ A kinetic-energy increase will appear as an apparent binding-energy decrease in the XPS spectrum. In terms of the average charge density $\bar{\rho}(z)$ over planes parallel to the interface, the dipole moment per unit area is

$$\tau = \int z\bar{\rho}(z) dz.$$

The self-consistent calculations of Baraff, Appelbaum, and Hamann⁶ and Pickett, Louie, and Cohen⁷ have shown that the potential variations near an interface are localized to within 1 or 2 atomic layers, a length considerably less than the Ge $3d$ and Ga $3d$ photoelectron escape depths.

Interface states and bulk doping differences which cause band bending can complicate the ability to determine ΔE_v from transport measurements. In the XPS techniques described here, however, because the photoelectron escape depth is much smaller than typical band-bending lengths \mathcal{L} ($\mathcal{L} > 10^3$ Å for moderate dopant levels), the effect of interface states is to shift the potential within the sampled region on both sides of an interface by the same constant value. Therefore, since ΔE_B is the difference in core-level binding energy for photoelectrons which originate from each side of the interface, any potential shift due to interface states or other sources of band bending cancel. It is assumed that the two semiconductors are nondegenerately doped and that the dimensions perpendicular to the interface sampled by XPS are small compared to \mathcal{L} .

The very thin (~ 20 -Å) epitaxial layers of Ge used for these interface studies were grown within the XPS apparatus on heated ($\approx 425^\circ\text{C}$) GaAs substrates by evaporative MBE techniques similar to those previously described,¹⁰ but at low flux rates. GaAs substrates with (100), (111), (111), and (110) faces were cut from a single boule of undoped GaAs (n -type carrier concentration 10^{16} cm⁻³).¹¹ Laue back-reflection photography showed that the substrates were oriented to better than 1° . Each substrate was etched in 3:1:1 H₂SO₄:H₂O₂:H₂O prior to insertion into the

XPS vacuum system. Substrate surfaces were cleaned by Ar^+ -ion sputtering (750 eV) followed by annealing at $\approx 575^\circ\text{C}$ to remove sputter damage (vacuum-system base pressure was low 10^{-10} Torr). Room-temperature low-energy electron-diffraction (LEED) patterns characteristic of (110) (1 \times 1), (111)Ga (2 \times 2), (111)As (1 \times 1), and (100)Ga c (8 \times 2) were obtained. In addition, a (100)As surface was also studied which was either c (2 \times 8) or (2 \times 4). Additional LEED measurements confirmed the epitaxy of the Ge overlayers. Following the XPS measurements, a metal point contact was made to the semiconductor surface to ensure reasonable diode characteristics.

Figure 2 shows an XPS spectrum from a sample of epitaxial Ge grown on a (110) (1 \times 1) GaAs substrate. To determine ΔE_B , a background function which is proportional to the integrated photoelectron area was subtracted from the data to correct for the effect of inelastic photoelectron scattering. ΔE_B was measured between the centers of the peak widths at half of the peak heights. This procedure made it unnecessary to resolve the spin-orbit splitting of the Ge 3*d* and Ga 3*d* lev-

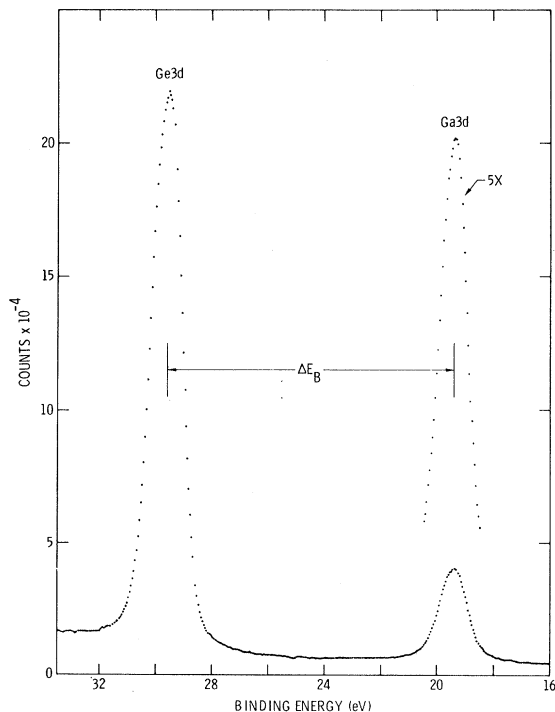


FIG. 2. XPS spectrum in the energy region of the Ga 3*d* and Ge 3*d* core levels obtained from a (110) Ge/GaAs interface. The thickness of the epitaxial Ge overlayer was ≈ 20 Å.

els (≈ 0.5 eV) to obtain high-precision peak positions.

Measurement results of eight different interfaces are given in Table I. In general, several (three to five) independent determinations were made on each interface. In all cases, measurement reproducibility was < 0.01 eV and was usually < 0.005 eV; calibration uncertainties increase the error limits to 0.1 eV. The measurements on the two samples of (110) (1 \times 1) and (111)As (1 \times 1) reproduce very well. We believe the discrepancy in the two values shown for (111)Ga (2 \times 2) is real and represents a subtle difference in the interface properties grown on this surface.

If we arbitrarily reference all $\delta(\Delta E_v)$ values to the (110) charge-neutral surface such that $\delta(\Delta E_v)_{110} \equiv 0$, we obtain the values of $\delta(\Delta E_v)$ shown in Table I. It is interesting that the (111)As and (111)Ga and the (100)As and (100)Ga differences are nearly symmetrically distributed around the (110) value. However, the known complexity of these surfaces¹² makes a simple interpretation of the variations in valence-band discontinuity difficult.

In summary, a technique has been developed to observe directly variations in band-gap discontinuities at abrupt semiconductor interfaces, and systematic changes in ΔE_v as a function of interface crystallographic orientation have been observed for Ge/GaAs. The maximum variation in ΔE_v between the (111) and (111) interfaces is ≈ 0.2 eV, which is a significant fraction ($\approx \frac{1}{4}$) of ΔE_g (0.75 eV). This result suggests that accurate future models used to predict ΔE_v and ΔE_c need to account for dipole orientation dependence.

We acknowledge helpful discussions with Profes-

TABLE I. Ge-3*d*-Ga-3*d* binding-energy differences and corresponding variations in valence-band discontinuity for various Ge/GaAs interfaces.

Substrate surface	ΔE_B (eV)	$\delta(\Delta E_v)$ (eV)
(111)Ga (2 \times 2)	10.27 ± 0.01	≈ -0.085
(100)Ga c (8 \times 2)	10.31 ± 0.01	
(110) (1 \times 1)	10.22 ± 0.01	-0.015
(110) (1 \times 1)	10.20 ± 0.01	0
(100)As	10.21 ± 0.01	
(100)As	10.17 ± 0.01	$+0.035$
...		
(111)As (1 \times 1)	10.11 ± 0.01	$+0.10$
(111)As (1 \times 1)	10.10 ± 0.01	

sor W. A. Harrison and appreciate the x-ray analysis performed by Dr. M. D. Lind. This work was supported by the U. S. Office of Naval Research, Contract No. N00014-76-C-1109.

¹R. L. Anderson, *Solid-State Electronic*, **5**, 341 (1962).

²H. Kroemer, *CRC Crit. Rev. Solid State Sci.* **5**, 555 (1975).

³J. L. Shay, S. Wagner, and J. C. Phillips, *Appl. Phys. Lett.* **28**, 31 (1976).

⁴W. A. Harrison, *J. Vac. Sci. Technol.* **14**, 1016 (1977).

⁵W. R. Frensley and H. Kroemer, *Phys. Rev.* **16**, 2642 (1977).

⁶G. A. Baraff, J. A. Appelbaum, and D. R. Hamann, *Phys. Rev. Lett.* **38**, 237 (1977), and *J. Vac. Sci. Technol.* **14**, 999 (1977).

⁷W. E. Pickett, S. G. Louie, and M. L. Cohen, *Phys. Rev. Lett.* **39**, 109 (1977), and to be published.

⁸F. F. Fang and W. E. Howard, *J. Appl. Phys.* **35**, 612 (1964).

⁹J. A. Stratton, *Electromagnetic Theory* (McGraw-Hill, New York, 1941), p. 190.

¹⁰R. F. Lever and E. J. Huminski, *J. Appl. Phys.* **37**, 3638 (1966).

¹¹Obtained from Morgan Semiconductor, Inc.

¹²See, e.g., W. Ranke and K. Jacobi, *Surf. Sci.* **63**, 33 (1977); A. Y. Cho, *J. Appl. Phys.* **47**, 2841 (1976); J. R. Arthur, *Surf. Sci.* **43**, 449 (1974); L. L. Chang, L. Esaki, W. E. Howard, R. Ludeke, and G. Schul, *J. Vac. Sci. Technol.* **10**, 655 (1973); several references to earlier work are contained in these papers.

Temperature Dependence of Transient Hole Hopping Transport in Disordered Organic Solids: Carbazole Polymers

G. Pfister and C. H. Griffiths

Xerox Webster Research Center, Webster, New York 14580

(Received 7 December 1977)

Nondispersive hopping transport has been observed in disordered poly(*N*-vinylcarbazole) (PVK) but not in the related polymer 3Br-PVK. The results demonstrate that a hopping-time distribution $\psi(t) \sim t^{-(1+\alpha)}$ can account for the transit-time dispersion in a limited temperature range but that more complicated $\psi(t)$'s are necessary to model the results in a broader temperature range. The subtle relation between sample morphology and transient dispersion is demonstrated.

The Scher-Montroll formalism¹ of continuous-time random walk (CTRW) successfully accounts for many novel features of dispersive (non-Gaussian) transport which, in some temperature range, is observed in time-of-flight experiments in most disordered solids.²⁻⁷ For *a*-As₂Se₃ transient hole transport remains dispersive over the entire experimental temperature range 230–380 K and its features can be explained with a CTRW based upon an event time distribution function $\psi(t) \propto t^{-(1+\alpha)}$ where the disorder parameter α assumes a value between zero and unity.^{1,2} The temperature insensitivity of the hole transit-time dispersion in *a*-As₂Se₃ requires $\alpha \sim \text{const.}$ ² It has been argued that a temperature-independent α indicates hopping rather than multiple-trapping transport and that the dominant source for the transit-time dispersion is associated with fluctuating hopping-site distances rather than a distribution of activation energies.^{1,2} In fact, a consistent numerical description of the transport data is obtained for trap-modulated hopping trans-

port² (trap-controlled hopping⁵).

Different temperature behavior is observed for transient hole transport in *a*-Se.³ The hole transients, which at room temperature are Gaussian, become progressively more dispersive as the temperature is lowered and below ~ 180 K approach the non-Gaussian features typical of *a*-As₂Se₃. Obviously a $\psi(t)$ more complicated than for *a*-As₂Se₃ is needed to account for these observations. That increase in complexity invariably leads to an increase of the number of adjustable parameters and, indeed, excellent agreement is obtained in terms of a generalized multiple-trapping formalism based on three traps (nine parameters).⁸ The latter formalism is mathematically equivalent to the CTRW theory.^{8,9} Interestingly the parameters derived from this model suggest a hopping process rather than transport in extended states.⁸ However, as for *a*-As₂Se₃, the identification of the microscopic transport process remains somewhat ambiguous.

While the analysis of the hole transit-time data